Buckling and kinking force measurements on individual multiwalled carbon nanotubes

K. Jensen, W. Mickelson, A. Kis, and A. Zettl
Department of Physics,and Center of Integrated Nanomechanical Systems, University of California at Berkeley, Berkeley, California 94720, USA
and Materials Sciences Division, Lawrence Berkeley National Laboratory, Berkeley, California 94720, USA
(Received 12 August 2007; published 26 November 2007)

Using an atomic force microscope operated inside a transmission electron microscope, we have studied the forces involved in buckling and kinking an individual multiwalled carbon nanotube while observing its structure. In particular, we have measured an individual nanotube's asymptotic critical buckling load and critical kinking load. The buckling results are well described by classical elastic theory, while the observed kinking behavior requires a more involved analysis. Repeated buckling measurements on the same nanotube indicate an extremely high degree of elasticity and set a lower bound on the nanotube's yield strength of 1.7 GPa, higher than the yield strength of steel. Plastic deformation of the nanotube was eventually observed following kinking.

DOI: 10.1103/PhysRevB.76.195436 PACS number(s): 62.25.+g, 61.46.Fg, 68.37.Ps, 68.37.Lp

I. INTRODUCTION

Carbon nanotubes are renowned for their remarkable mechanical properties, which include exceptionally high axial elastic modulus and tensile strength.[1–3] Because of such advantageous properties, nanotubes have been suggested as components in mechanical systems ranging from atomic force microscope (AFM) tips[4] to resilient composites[5] to stronger-than-steel cables[6,7] (such as those critical to space elevator applications).[8] All of these applications, including those employing collections of nanotubes, would benefit greatly from a better understanding of the mechanical behavior of *individual* nanotubes. While the elastic modulus and tensile strength of individual nanotubes have been well characterized by multiple techniques,[1–3,9] an equally important property, the critical buckling load is comparatively less well understood. Thus, we here study the buckling behavior of individual, isolated multiwalled carbon nanotubes (MWNTs).

Buckling is the failure of a structural component under an excessive compressive load. Obviously, this effect is critical on the macroscopic scale where it is a principal consideration in the design of structural members for buildings and bridges, but it is also important on the nanoscale where, for example, it governs the behavior of nanotube-tipped AFM cantilevers or determines whether a nanotube can penetrate a cell's membrane.[10]

Two distinct forms of buckling, one simply termed "buckling" and the other termed "kinking," are discussed in this paper. Simple buckling, depicted in Fig. 1(b), occurs when the nanotube no longer remains straight under a compressive load. In this case, a relatively constant curvature develops along the entire length of the nanotube. Kinking, a more drastic form of buckling depicted in Fig. 1(c), occurs when the compressive load increases until a sharp bend forms at one point along the length of the nanotube.

In our experiment, we measure the forces involved in buckling and kinking an individual, isolated MWNT. Our approach has distinct advantages over previous nanotube buckling experiments.[11–14] Most importantly, we observe the MWNT's geometry with nearly atomic resolution while measuring the forces involved. Also, we avoid interference in the force measurements from a substrate or embedding matrix through meticulous control of the experiment's geometry. Finally, we can repeat the experiment on the same nanotube to look for possible permanent structural changes.

II. EXPERIMENT

The experimental requirements for measuring the forces involved in buckling and kinking a single MWNT while observing its geometry are demanding. To precisely measure the forces, an AFM would be ideal. However, to observe the MWNT geometry, including the structure of the inner nanotubes, with atomic resolution, a transmission electron micro-

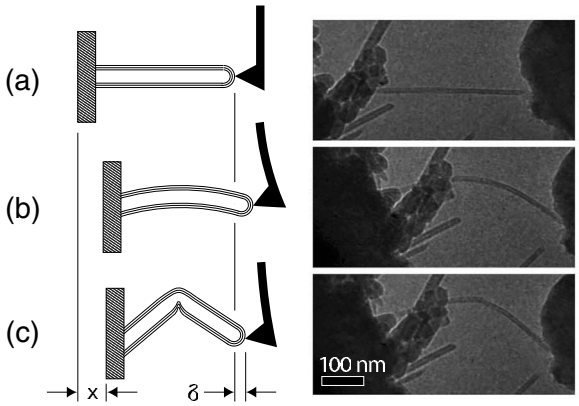

FIG. 1. Schematic of a buckling and kinking force measurement along with corresponding TEM video frames of the measurement in progress. (a) Straight nanotube. A single MWNT protrudes from the translator on the left and contacts an AFM cantilever on the right. The AFM cantilever shows no deflection and thus there is no applied compressive force. (b) Buckled nanotube. As the translator moves to the right, the nanotube pushes against the AFM cantilever. In return, the AFM cantilever applies a compressive force to the nanotube, which causes it to buckle. (c) Kinked nanotube. Further rightward translator movements cause the nanotube to kink, or locally buckle, which reduces the compressive force sustained by the nanotube.

scope (TEM) is necessary. Finally, to manipulate the nanotube at the nanoscale in order to control the buckling process, a nanopositioning platform is required. We satisfy all of these requirements by outfitting a commercial TEM nanopositioning system (Nanofactory Instruments AB) with a standard AFM cantilever.

The initial configuration of our experimental setup is shown schematically in the left half of Fig. 1(a). On the left side of the schematic is the piezoelectric translator of the nanopositioning system. The MWNT to be characterized is attached to this translator. On the right side of the schematic is the AFM cantilever, which is placed on the stationary (relative to the microscope) side of the nanopositioning system in an orientation such that the cantilever is deflected in the plane that forms the TEM image. Importantly, both the MWNT and AFM cantilevers are electrically grounded to prevent charging from the TEM's electron beam. At the start of an experiment, the MWNT is positioned using the translator so that it contacts, but does not deflect, the AFM cantilever. Through the course of an experiment, the translator extends and retracts, causing the nanotube to go through various stages of buckling and kinking. The entire experiment is conducted at room temperature inside a JEOL-2010 TEM and recorded with a Gatan 794 charge-coupled device video camera.

In a typical experiment, the geometry of the MWNT progresses through three stages: straight, buckled, and then kinked. These stages are shown schematically in the left column of Fig. 1. At the start of the experiment, the MWNT is straight, as shown in Fig. 1(a). There is no force on the nanotube, and thus the AFM cantilever shows no deflection. As the translator extends to the right by distance x, the nanotube displaces the AFM cantilever on the right by distance δ. In return, the AFM cantilever applies a compressive force $F=-k_{\mathrm{eff}}\delta$ to the nanotube, where k_{eff} is the effective spring constant of the AFM cantilever. This compressive force eventually causes the nanotube to buckle, as shown in Fig. 1(b). By further moving the translator to the right, it is possible to steadily increase the force applied to the already buckled nanotube. Finally, at some critical load, a sharp bend or kink forms along the nanotube, as shown in Fig. 1(c).

An experiment does not necessarily end once the nanotube kinks. Afterward, it is possible to retract the translator and relieve the force on the nanotube. The kink in the nanotube will disappear and the nanotube will relax to its unloaded, straight configuration. The experiment may be repeated multiple times on the same nanotube to confirm the critical buckling and kinking forces or to test for permanent structural damage inflicted on the nanotube by the buckling or kinking.

The right column of Fig. 1 shows TEM video frames from an experiment in progress. The chosen frames correspond to the straight, buckled, and kinked geometries shown schematically in the left column. As in the schematics, the translator is on the left, and the tip of the AFM cantilever appears on the right.

One notable difference between the video frames and the schematics is that the translator appears much "dirtier" in the video. This is due to our method of attaching the MWNT. In fact, we do not attach a single MWNT to the translator, but rather for reasons of practicality, we attach a macroscopic mat of many MWNTs with epoxy. All force measurements are made on a particular nanotube that protrudes far from the mat. Unfortunately, this technique somewhat obscures the translator-side attachment of the nanotube; however, as will be discussed later, this does not pose significant problems.

There is a wealth of information regarding the buckling process contained in the TEM video. Most importantly, it is easy to quantify the displacements of both the translator and the AFM cantilever. We note, for example, that the AFM tip deflects to the right more when the nanotube is buckled [Fig. 1(b)] than when it is kinked [Fig. 1(c)], indicating that a kinked nanotube supplies less force. It is straightforward to measure basic properties of the MWNT such as its inner and outer diameters and its length. Moreover, the shape of the buckled nanotube, the location and angle of the kink, and the way the nanotube contacts the AFM tip are all clearly visible. Such detailed information about the MWNT's geometry has not been available in previous experiments,[11–14] and these data now facilitate a much more accurate analysis of MWNT buckling.

The first step in analyzing the buckling and kinking data is to determine the force supplied by the MWNT through the various stages of buckling and kinking. In our experimental setup due to the restrictive geometry of the TEM, forces are not read from the AFM using one of the standard techniques.[15] Rather, as mentioned earlier, it is possible to directly measure the deflection of the AFM cantilever by imaging it with the TEM itself. Here, an image processing routine analyzes the recorded TEM video to find the deflection of the cantilever. This deflection is converted to a force via the effective spring constant of the cantilever ($k_{\mathrm{eff}}=0.3$ N/m, calibrated using the method of Sader *et al.*).[16] A similar system has been successfully used to measure forces in other experiments that demand the atomic resolution of the TEM, such as measuring the interlayer forces between telescoping nanotubes.[17] In this experiment, we use this technique to achieve force sensitivities on the order of 180 pN.

Using the image processing routine, we found the compressive force applied to the nanotube and the translator position through the course of a typical experiment. These are shown in the top and bottom plots, respectively, of Fig. 2. The nanotube begins in the unbuckled state shown in Fig. 1(a), but it becomes slightly buckled as soon as the translator moves. In the first section, the translator slowly moves in steps to the right. At first, each translator step results in significant increases in compressive force, on the order of 4 nN. However, the first step after the 16 s mark results in a smaller increase in force around 1 nN, and the following two steps result in no significant increase in force. Thus, as the nanotube becomes more buckled, the force it supplies approaches a constant value.

In the next section, the translator again slowly moves to the right until the compressive force reaches 13.5 nN and the nanotube kinks [Fig. 1(c)]. Within the time span of a single TEM video frame (33 ms), the force supplied by the nanotube decreases, 1.7 nN. This sudden decrease in force is indicative of an elastic instability. Over the next 2 s, while the translator remains stationary, the force continues to decrease by another nanonewton, indicating some form of relaxation

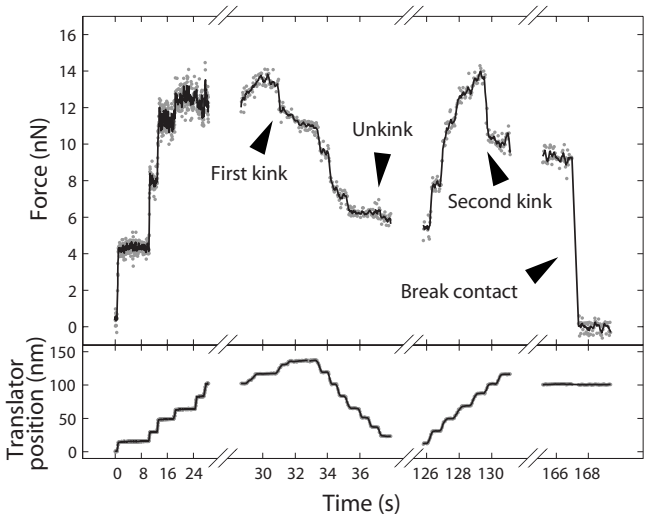

FIG. 2. Force measurements on a buckled and then kinked nanotube over the course of a typical experiment. The top plot shows the force supplied by the nanotube as it progresses through various stages of buckling and kinking. Note the rapid decrease in supplied force following a kink. The bottom plot shows the position of the translator, which extends or retracts to control the buckling or kinking. In order to clarify the presentation, the first section uses a different time scale.

process. The translator then retracts until the nanotube unkinks, which interestingly results in only a very small change in force.

In the third section, the experiment was repeated on the same nanotube. The translator was again moved to the right, and the force supplied by the nanotube followed a similar curve and kinked in the same position and at almost the same force, 13.8 nN. However, this kink resulted in a significantly larger sudden decrease in force, 2.7 nN, possibly indicating that the slow relaxation of the previous kink resulted in permanent changes to the nanotube's structure.

In the last section of Fig. 2, the contact between the nanotube and the AFM tip was broken. This allowed the cantilever to relax to its neutral position, which defines the base line for zero force.

III. ANALYSIS

The first two sections of our analysis, Secs. III A and III B, use the classical elastic theory, where the MWNT is modeled as a continuum elastic medium, to explain many of the experimental results. Section III A uses Euler's theory of buckling to describe the forces produced during simple buckling. Fitting this model to our experimental data yields the critical buckling load and Young's modulus of the MWNT. Section III B uses Brazier's theory of buckling, which includes the effect of a deformable cross section, to describe the process of kinking and provide a close lower bound for the critical kinking moment of the MWNT, which is consistent with our experimental data.

The last section of our analysis, Sec. III C, discusses the limits of elasticity in MWNTs. Here, we calculate a lower limit to the yield strength of MWNTs and present evidence for permanent changes in the atomic structure of the MWNT following the first kink.

A. Euler buckling

Euler was the first to give an analytical model of buckling, and although his model is simplistic, it contains many of the features of more advanced models. In the Euler model, there is an initially straight, uniform, elastic beam with Young's modulus E and areal moment of inertia I, which is under a compressive force F from the ends. According to the elastic theory of beams, the deflection, $y(x)$, of the beam from its initially straight configuration is described by the differential equation[18]

$$EI\frac{d^4y}{dx^4} + F\frac{d^2y}{dx^2} = 0. \tag{1}$$

For small loads, this model only permits the trivial solution $[y(x)=0]$ or a perfectly straight column. However, when the load is increased to some critical load, F_{cr}, a situation known as an elastic instability occurs where there are two solutions, the straight column solution and the buckled solution. The straight column solution is unstable to small perturbations in y; hence above F_{cr}, the column buckles.

The value of the critical buckling load depends on how the nanotube is attached to its supports. It is clear from Fig. 1 that the attachment on the right may be described as a pin joint because the angle of the nanotube relative to the surface is variable. The attachment on the left, however, is somewhat obscured. To discern the type of attachment, we extend lines tangent to the nanotube as it disappears behind the substrate for multiple frames of the video. These lines converge approximately to the same point, again indicating a pin joint and also revealing the approximate location of the attachment. Now, Eq. (1) can be solved using the boundary conditions for a doubly pin-jointed beam of length L $[y(0)=0, y(L)=0, y''(0)=0, y''(L)=0]$ to give a critical buckling load of $F_{cr}=\pi^2EI/L^2$.

Euler's model is a great simplification. If it were to hold true, we would expect a sharp, discontinuous initial increase in force as the translator was first moved causing the nanotube to buckle, and then relatively small changes in force as the translator was moved further. As can be seen in the first and third sections of Fig. 2, the increase in force is continuous and only begins to taper off after the translator has moved more than 100 nm. The problem lies in the fact that the nanotube is not, strictly speaking, a perfectly straight column, which can be seen by closely examining Fig. 1(a).

To extend Euler's model to account for initially slightly crooked columns, we assume that the column has an initial shape, $y_0(x)$ and a deflection from this shape of $y_1(x)$. Equation (1) is modified to give[18]

$$EI\frac{d^4y_1}{dx^4} + F\frac{d^2}{dx^2}(y_0 + y_1) = 0. \tag{2}$$

For simplicity, we assume that $y_0(x)$ has the form $A\sin(\pi x/L)$. Note that a more complicated, empirical form

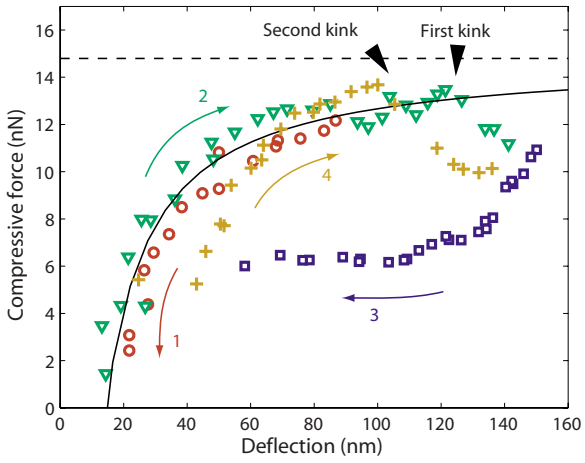

FIG. 3. (Color online) Compressive force applied to a nanotube versus the maximum deflection from a straight configuration for a buckled and then kinked nanotube over multiple cycles. The data before the kinks are well described by Euler's theory of buckling applied to an initially slightly crooked column. A fit to this model is shown by the solid line. The horizontal dashed line represents a parameter of this fit, the asymptotic critical buckling load.

determined from TEM micrographs [Fig. 1(a)] yields similar results. This more realistic model has the solution

$$y = y_0 + y_1 = \frac{A}{1 - F/F_{\mathrm{cr}}} \sin(\pi x/L), \tag{3}$$

which allows small deflections for small loads. However, as the load increases toward F_{cr}, the critical load for Euler's simple model, the deflection again diverges.

As suggested by these models, in Fig. 3, we replot the data from Fig. 2 (along with more data for the same nanotube, which was not shown in Fig. 2) as compressive force versus maximum displacement. The data are grouped into four sweeps: an initial outward sweep to straighten the nanotube, the first inward sweep and the first kink, another outward sweep with the nanotube in its kinked configuration, and a second inward sweep to repeat the experiment.

The portion of the data where the nanotube is not kinked (i.e., sweep 1 and the first portions of sweeps 2 and 4) is well described by Euler's model with the initially slightly crooked column. We fit this model, as described by Eq. (3), to the data from sweep 1 and the first portion of sweep 2 using the amplitude of y_0 and the critical buckling load as fitting parameters. From the fit, we determine $A=14.4$ nm and $F_{\mathrm{cr}}=14.8$ nN.

From the fitted value of the critical load and from the length and inner and outer diameter measurements of the nanotube from the TEM video images, it is possible, using Euler's formula for the critical load, to determine a value for Young's modulus of the nanotube. Using the values $F_{\mathrm{cr}}=14.8$ nN, $L=610$ nm, $D=12.8$ nm, and $D_i=3.2$ nm, we find that $E=425$ GPa. This value is consistent with previous measurements of Young's modulus for MWNTs obtained with alternate techniques.[19]

B. Brazier theory and local buckling

In Euler's theory of buckling, it is assumed that the cross section of the column remains constant throughout the buckling process. This is not necessarily true and, moreover, a deformable cross section has significant effects on buckling. As a cylindrical tube is bent, its cross section changes from circular to elliptical, most dramatically at its midpoint where the curvature and thus the bending moment are greatest. The change in cross section decreases the tube's flexural stiffness, making it progressively easier to bend or more specifically reducing the *additional* bending moment required to induce a unit change in curvature. This implies that there is a maximum bending moment that the tube can withstand. Beyond this point, the tube buckles locally, or kinks, where the bending moment is greatest, again at the center. Both the decrease in flexural stiffness and the kinking are effects not found in Euler's original theory of buckling.

Brazier studied these effects for the case of a *thin-walled* tube with an initially circular cross section.[20] He calculated the maximum moment that the tube could withstand, or the critical kinking moment, to be[21]

$$M_{kink} = 0.4683 \frac{EDt^2}{\sqrt{1-\nu^2}}. \tag{4}$$

Here, t is the thickness of the tube and ν is the Poisson ratio of the tube's material ($\nu=0.17$ for graphite[22]).

Many MWNTs, including the one used in this study, are not necessarily "thin walled" as their thickness is a significant portion of their total radius. Nonetheless, the Brazier theory provides a useful lower bound for their expected critical kinking moment. This lower bound is determined by considering only the outermost shells of a thick MWNT, which do form a thin tube. Clearly, the critical kinking moment of the entire, thick MWNT will be greater than this bound as the inner shells can only impede the formation of a kink. For the approximations used in the Brazier theory to hold, the thickness of these outer shells must be significantly less than the MWNT's radius. For the particular MWNT used in our experiment, considering only the outer two shells and using the fitted value for E, the lower bound for the critical kinking moment is 1200 nN nm. The measured critical kinking moment, as determined from Fig. 3, rests slightly above this limit, as expected, at 1600 nN nm.

C. Plastic deformation

Before the MWNT kinks, it displays, to within the precision of our instrument, a completely elastic behavior. This is easily seen in Fig. 3 by considering that paths 1 and 2 coincide. Interestingly, we can use this fact to calculate a lower bound for the yield strength of MWNTs of 1.7 GPa, which is greater than the yield strength of steel.[23] However, after the first kink, there is evidence that the MWNT has been plastically deformed, which means that there have been permanent changes to its atomic structure.

First, it should be noted that the hysteresis in the force versus deflection curve of Fig. 3 is not, by itself, an indication of plastic deformation. This particular inelastic behavior

occurs because of the rapid transition between configurations with different strain energies during a kink. The excess energy is dissipated through vibrations and heat and not, necessarily, through rearrangements in atomic structure.

Rather, evidence for plastic deformation comes from the slightly different force versus deflection curve of path 4 when compared to paths 1 and 2. The curve of path 4 indicates that the neutral shape of the MWNT, after the first kink, has become more crooked. As was done with paths 1 and 2, we fit the model described in Eq. (3) to path 4, and from the fit, we determine that there was a larger initial deflection of 30 nm. Obviously, a change in the neutral shape of the MWNT must be due to changes in the atomic structure.

More evidence for plastic deformation comes from the critical bending moment of the second kink. While the second kink occurs at the same position along the nanotube and at approximately the same compressive force, it occurs at a significantly lower bending moment. The change in critical bending moment must be due to a local (i.e., near the kink) change in one of the parameters of Eq. (4) or to a flattening of the cross section of the nanotube at the kink, both due to changes in atomic structure.

It is still an open question as to what mechanism governs the atomic rearrangements. Some changes in atomic structure likely occur immediately following or even during the kinking process. Quick atomic rearrangements as a result of kinking have been predicted by molecular dynamics simulations.[24] Other changes appear to occur over longer periods of time. Shortly after the first kink, there is, as shown in Fig. 2, a period where the force supplied by the MWNT slowly relaxes over the span of 2 s. This could be explained by the thermally assisted migration of defects, either inherent to the nanotube or created by the 100 keV electron beam of the TEM, to the area of the kink.

IV. CONCLUSION

Using our technique for operating an AFM inside a TEM, we have thoroughly studied the forces involved in repeatedly buckling and kinking a single MWNT and correlated them with the geometry of the MWNT. Specifically, we have precisely measured the compressive force sustained by a buckled and then kinked, or locally buckled, MWNT as a function of its deflection from an initial state. These measurements are in good agreement with the classical elastic theory of buckling. Moreover, the value of Young's modulus for a MWNT determined by these measurements is consistent with values obtained by alternate techniques. Finally, by repeatedly buckling and kinking a MWNT, we have tested the limits of its elasticity and set a lower bound on its yield strength.

ACKNOWLEDGMENTS

This work was supported primarily by the Director, Office of Energy Research, Office of Basic Energy Sciences, Materials Sciences Division of the U.S. Department of Energy under Contract No. DE-AC-03-76SF00098. K.J. acknowledges support by the Center of Integrated Nanomechanical Systems and A.Z. acknowledges support by the Miller Institute for Basic Research in Science.

[1] B. G. Demczyk, Y. M. Wang, J. Cumings, M. Hetman, W. Han, A. Zettl, and R. O. Ritchie, Mater. Sci. Eng., A **334**, 173 (2002).
[2] M. M. J. Treacy, T. W. Ebbesen, and J. M. Gibson, Nature (London) **381**, 678 (1996).
[3] M. F. Yu, O. Lourie, M. J. Dyer, K. Moloni, T. F. Kelly, and R. S. Ruoff, Science **287**, 637 (2000).
[4] H. J. Dai, J. H. Hafner, A. G. Rinzler, D. T. Colbert, and R. E. Smalley, Nature (London) **384**, 147 (1996).
[5] L. S. Schadler, S. C. Giannaris, and P. M. Ajayan, Appl. Phys. Lett. **73**, 3842 (1998).
[6] A. B. Dalton, S. Collins, E. Munoz, J. M. Razal, V. H. Ebron, J. P. Ferraris, J. N. Coleman, B. G. Kim, and R. H. Baughman, Nature (London) **423**, 703 (2003).
[7] M. Zhang, K. R. Atkinson, and R. H. Baughman, Science **306**, 1358 (2004).
[8] B. C. Edwards, Acta Astron. **47**, 735 (2000).
[9] E. W. Wong, P. E. Sheehan, and C. M. Lieber, Science **277**, 1971 (1997).
[10] X. Chen, A. Kis, A. Zettl, and C. R. Bertozzi,Proc. Natl. Acad. Sci. U.S.A. **104**, 8218 (2007).
[11] J. F. Waters, L. Riester, M. Jouzi, P. R. Guduru, and J. M. Xu, Appl. Phys. Lett. **85**, 1787 (2004).
[12] J. F. Waters, P. R. Guduru, M. Jouzi, J. M. Xu, T. Hanlon, and S. Suresh, Appl. Phys. Lett. **87**, 103109 (2005).
[13] M. R. Falvo, G. J. Clary, R. M. Taylor, V. Chi, F. P. Brooks, S. Washburn, and R. Superfine, Nature (London) **389**, 582 (1997).
[14] O. Lourie, D. M. Cox, and H. D. Wagner, Phys. Rev. Lett. **81**, 1638 (1998).
[15] G. Meyer and N. M. Amer, Appl. Phys. Lett. **53**, 1045 (1988).
[16] J. E. Sader, I. Larson, P. Mulvaney, and L. R. White, Rev. Sci. Instrum. **66**, 3789 (1995).
[17] A. Kis, K. Jensen, S. Aloni, W. Mickelson, and A. Zettl, Phys. Rev. Lett. **97**, 025501 (2006).
[18] S. Timoshenko and J. Gere, *Theory of Elastic Stability* (McGraw-Hill, New York, 1961).
[19] D. Qian, G. J. Wagner, W. K. Liu, M.-F. Yu, and R. S. Ruoff, Appl. Mech. Rev. **55**, 495 (2002).
[20] L. G. Brazier, Proc. R. Soc. London, Ser. A **116**, 104 (1927).
[21] C. R. Calladine, *Theory of Shell Structures* (Cambridge University Press, Cambridge, 1983).
[22] O. L. Blakslee, D. G. Proctor, E. J. Seldin, G. B. Spence, and T. Weng, J. Appl. Phys. **41**, 3373 (1970).
[23] J. Shackelford and W. Alexander, *CRC Materials Science and Engineering Handbook, 3rd Ed.* (CRC, Boca Raton, FL, 2001).
[24] Y. Shibutani and S. Ogata, Modell. Simul. Mater. Sci. Eng. **12**, 599 (2004).